Optimization of a simulated iron-oxide pellets induration furnace

Dominique Pomerleau[1], André Desbiens[2] and Daniel Hodouin[3]

***Abstract*-- Induration furnaces for iron-oxide pellets are expensive processes, due to their high energy consumption. Moreover, they are highly interactive and then complex to control. Real-time optimization strategies based on reliable process models are thus necessary. However, induration furnaces are described by distributed-parameter models that require long computation times. The performance of IMC-optimization [1], an easy to implement static nonlinear optimization algorithm, is compared to a direct optimization based on the nonlinear process model itself. For a simulated induration furnace, it is shown that the accuracy obtained with the IMC-optimization algorithm is quite sufficient and does not require considerable computation efforts.**

***Index terms*—Optimization, IMC, Induration furnace**

I. Introduction

In a context of sharp competition and equipment overexploitation, the ultimate plant management objective is to increase process efficiency, i.e. increase levels of production, reduce operating costs, and improve product quality control. The implementation of a real-time optimization (RTO) system is a convenient approach to this problem. RTO consists of finding and modifying the operating conditions in order to maintain a maximum economic productivity [2].

In the last twenty years, iron-making companies have increased their research activities to reduce energy consumption [5]. Moreover, the product specifications required by the clients are becoming more difficult to achieve and the implementation of RTO strategies can then be advantageous to remain competitive on the international scene. However, the first principles model of an induration furnace, the most critical production equipment of a pelletizing plant, requires important computation times since it is a distributed parameter system which can hardly be simplified while keeping good prediction capabilities. Consequently, first principles models cannot be easily implemented on-line in RTO strategies. Thus, the aim of this paper is to evaluate the performance of a new algorithm for steady-state optimization of an iron-oxide pellet induration furnace .

Several powerful optimization techniques exist [3]. When the model used to define the process behavior is linear, the minimization of the performance index is usually easy, even in presence of constraints. However, if the model is nonlinear, more efficient algorithms are needed. Their implementation and tuning may sometimes be difficult. Furthermore, the calculation time may be too long for real time implementation. To reduce the computation time required to optimize complex processes, Desbiens and Shook [1] proposed an easy to implement optimization algorithm which is based on the internal model controller (IMC) structure [4]. The optimization relies on an approximate reduced model of the nonlinear process. The steady-state reached when running the IMC structure is an approximate solution to the optimization problem. The optimization algorithm, which is simple to tune and to implement, rapidly converges to an optimum. The IMC-Optimization scheme is particularly interesting for processes that are described with models requiring long computation time.

The next section briefly describes the IMC-optimization algorithm. Section 3 presents the induration furnace, its first principles model, and the optimization objectives. The results of the IMC-optimization algorithm application to a simulated induration furnace are given in Section 4. Finally, the study conclusion is presented in Section 5.

II. IMC-Optimization algorithm

The algorithm used for nonlinear optimization is based on the internal model control structure designed using a reduced steady-state model of the process. Finding an optimum consists in running the procedure depicted in Fig. 1 until convergence. During the iteration process the optimization steps k play the same role as the sampled control times of an internal model controller. At each step (or control time) k, a cost function that depends on a reduced model is minimized. Consequently, simple algorithms, such as quadratic programming, are adequate to

[1] Swabey Ogilvy Renault, 500 Grande-Allée Est, Bureau 520 Québec, Québec, Canada, G1R 2J7
[2] Department of Electrical and Computer Engineering
[3] Department of Mining, Metallurgical and Material Engineering
LOOP (Laboratoire d'observation et d'optimisation des procédés – Process Observation and Optimization Laboratory)
Pavillon Adrien-Pouliot,
Université Laval, Quebec City, Quebec, Canada G1K 7P4
E-mail: dpomerleau@ogilvyrenault.com

solve the problem. Corrections are calculated by the means of the IMC feedback structure. Even in presence of a large model mismatch, constraints are respected. The convergence is usually faster than a direct optimization based on the nonlinear model itself.

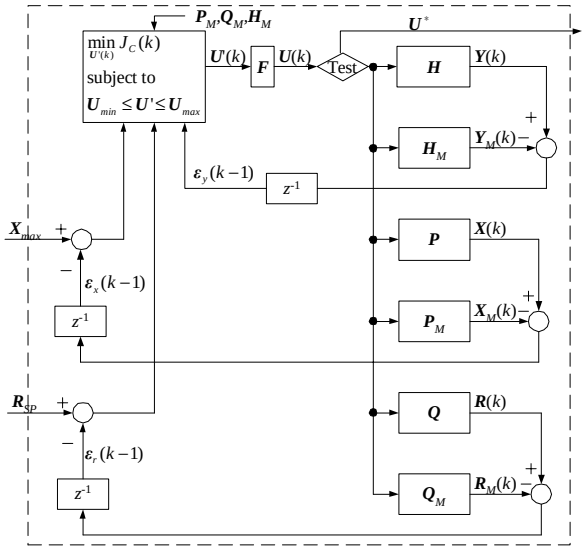

Figure 1: IMC-Optimization structure.

The steady-state and nonlinear process model is represented by the operator $\boldsymbol{H}$ which acts on the independent variables $\boldsymbol{U} \in \Re^{n_u}$ to produce the dependent variables $\boldsymbol{Y} = (\boldsymbol{HU}) \in \Re^{n_y}$. The cost function to be minimized is

$$J = f(\boldsymbol{Y}, \boldsymbol{U}) \qquad (1)$$

The optimization is subject to the following constraints:

$$\begin{aligned} \boldsymbol{X} &\le \boldsymbol{X}_{max} \\ \boldsymbol{R} &= \boldsymbol{R}_{SP} \end{aligned} \qquad (2)$$

where $\boldsymbol{X} = (\boldsymbol{PU}) \in \Re^{n_x}$ and $\boldsymbol{R} = (\boldsymbol{QU}) \in \Re^{n_R}$ are some states of the process which are respectively obtained by applying the static nonlinear operators $\boldsymbol{P}$ and $\boldsymbol{Q}$ to $\boldsymbol{U}$.

The operators $\boldsymbol{H}$, $\boldsymbol{P}$, and $\boldsymbol{Q}$ being possibly highly nonlinear and requiring large computation efforts, the minimization of Eq. (1) subject to Eq. (2) may be difficult and time consuming. The IMC structure facilitates and accelerates the optimization. The solution is obtained by simulating Fig 1 until convergence. The operators $\boldsymbol{H}$, $\boldsymbol{P}$, and $\boldsymbol{Q}$ are only needed to calculate corrections through the IMC structure. The cost function J_C is optimized using simpler operators $\boldsymbol{H}_M$, $\boldsymbol{P}_M$, and $\boldsymbol{Q}_M$ which may even be linear. The cost function $J_C(k)$ at step k of the simulation is

$$J_C(k) = f(\boldsymbol{Y}_M(k) + \boldsymbol{\varepsilon}_y(k-1), \boldsymbol{U}'(k)) \qquad (3)$$

and the constraints at the step k are

$$\begin{aligned} \boldsymbol{X}_M(k) &\le \boldsymbol{X}_{max}(k) - \boldsymbol{\varepsilon}_x(k-1) \\ \boldsymbol{R}_M(k) &= \boldsymbol{R}_{SP}(k) - \boldsymbol{\varepsilon}_r(k-1) \end{aligned} \qquad (4)$$

The optimization of J_C at step k leads to the optimal value $\boldsymbol{U}'(k)$ which is subsequently filtered by the function $\boldsymbol{F}$ which is used to accelerate or decelerate the move towards the solution. Usually, $\boldsymbol{F}$ is a first-order low-pass filter defined by the tuning parameter ρ $(0 \le \rho \le 1)$

$$\boldsymbol{F} = \frac{(1-\rho)}{(1-\rho z^{-1})}\boldsymbol{I} \qquad (5)$$

The mathematical proofs that the constraints (2) are respected and a discussion on the stability and optimality are presented in Desbiens and Shook [1].

In order to have signals with approximately all the same magnitude, all variables are normalized and the operation points are removed as follows

$$\upsilon^n = \frac{\upsilon}{\upsilon_{op}} - 1 \qquad (6)$$

where υ is the signal expressed in engineering units, υ^n is the normalized signal, and υ_{op} is its operating point (nominal value).

When implementing the proposed structure, the iteration process is stopped when $\left\| \boldsymbol{U}(k) - \boldsymbol{U}(k-1) \right\|_2 \le \eta\sqrt{n_u}$, where η>0. The parameter η is therefore the desired precision for the elements of the solution $\boldsymbol{U}$, equivalent to the termination tolerance for usual optimization algorithms. It is important to select a value of the parameter η consistent with the nonlinear process model accuracy.

III. Process: Induration Furnace

The preparation of iron ore concentrates for iron and steel-making industries usually requires stages of ore concentration and agglomeration of iron oxide pellets. The agglomerated pellets are sintered in an induration furnace in order to give them the necessary mechanical properties for their handling and transportation to the reduction site.

Several complex phenomena occur during the sintering process such as the pellet drying, hardening (or cooking) and cooling, the coke combustion, the magnetite oxidation, and the limestone calcination. The moving grate furnace

can be divided into seven zones, as shown in Fig. 2 : the upwards drying (UD), the downwards drying (DD), the pre-cooking (PC), the first cooking (cooking 1), the second cooking (cooking 2), the first cooling (cooling 1), and the second cooling (cooling 2) zones. In Fig. 2, thick lines indicate pellet flows, while thin lines identify gas streams. The water contained within the agglomerated pellets is evaporated in the upwards and downwards cooling zones. The pellet sintering starts in the pre-cooking and is accelerated in the first and second cooking zones. Finally, the pellets are cooled down in the two cooling zones in order to recycle the energy for the drying and cooking zones and to obtain pellets at a suitable temperature for subsequent handling. To maximize the energy efficiency of the process, the pellets and the gas circulate in a counter-current way. Five fans are used to force the gas flows within the induration furnace. In Fig. 2, fans are symbolized by circles and are numbered V_1 to V_5 . Burners are located in the three cooking zones and are symbolized by ovals. $F_{m,PC}$, $F_{m,C1}$ and $F_{m,C2}$ represent the fuel flow in each zone. The letters T and P respectively represent temperature and pressure sensors. In the induration furnace, thermocouples are used to measure the gas temperatures. The differential pressures between the furnace and the atmospheric pressure are measured by pressure gauges and are also important controlled variables. No sensor exists to measure on-line the pellet temperature.

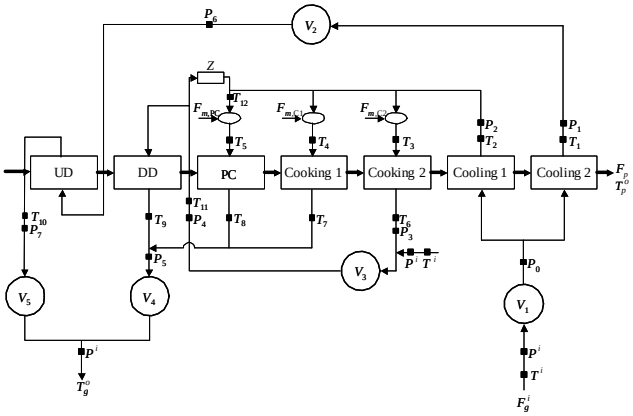

Figure 2: Induration furnace scheme.

A. *First principles model*

Although the literature abounds in studies related to the modeling of the pellet bed phenomena [6-7], works integrating all the complexity of the process, as in the present case, are almost inexistent [8].

The gas flow distribution within a pellet induration system can be described by a network of streams and nodes. A stream is a component, such as a duct, that have a single flow rate which is essentially governed by the pressure gradient at the nodes at either end of the stream. The nodes are simply the points where two or more streams meet. In such a network, there are well-established physical constraints and laws that have to be obeyed:

1. Kirchoff's first law: the sum of the flows into and out from a node is zero.
2. Kirchoff's second law: the pressure around any closed loop in the network is zero.
3. There is a single pressure at each node.

The model itself essentially relates the pressure drop across a component or stream to the flow rate through it. The pressure drop in the packed bed is calculated from the Ergun's model where only the turbulent part is considered [7]:

$$\frac{dP}{dz} = \frac{1.75(1-\varepsilon)}{\xi^2 d\varepsilon^3 \rho_g} \dot{F}_g^2 \qquad (7)$$

where dP is the pressure variation, z the height, ε the bed permeability, ρ_g the gas density, d the pellet diameter, $\dot{F}_g^2$ the superficial airflow rate, and ξ the pellet sphericity.

For a given gas density, fans are characterized by their static pressure-flowrate and power curves provided by the manufacturer. Both curves are modeled by third order polynomials. The fan pressure variation (dP) is inversely proportional to the density for a given volumetric flowrate (Q_g) [9]:

$$dP = \frac{\rho_g}{\rho_{g,ref}} (\alpha_1 Q_g^3 + \alpha_2 Q_g^2 + \alpha_3 Q_g + \alpha_4) \qquad (8)$$

where α_i are coefficients determined from the manufacturer data and $\rho_{g,ref}$ the gas density at the reference temperature at which the fan curve was identified. The power consumed (W_V) by each fan is calculated by the equation given by Azfal and Cross [10] which is based on the first thermodynamic principle:

$$W_V = \frac{F_g RT}{\eta_V M_g} \ln(dP) \qquad (9)$$

where R is the gas constant, η_V the fan efficiency, and M_g is the gas molar weight.

Leakages are not simulated since they are negligible comparatively to the gas streams. Pressure drops in ducts are neglected since they are relatively small in comparison to pressure drops within the pellet bed, except in a critical part of the furnace where the pressure loss is given by:

$$dP = ZQ_g^2 \qquad (10)$$

where Z is an empirical parameter which is a function of the gas temperature.

The packed bed of solid pellets is split up into a two-dimensional array of (m,n) cells each having a width dx and a height dz as shown in Fig. 3. Each cell is considered as an independent elementary thermal storage unit in which time-independent convective heat transfer occurs. The heat conduction between and inside the pellets was neglected as in the steady-state simulator proposed by Ekongolo et al. [8]. An energy balance is done for each cell. The energy equations are written assuming that gas and solid temperatures vary only in the flowing directions, horizontally for the solids (x axis) and vertically for the gas (z axis). For one cell with a height dz having a dry superficial pellet flow $\dot{F}_p$ subject to a superficial gas flow $\dot{F}_g$, the energy balance for the gaseous phase is:

$$\underbrace{h\ddot{A}_p(T_g - T_p)}_{\text{Convective heat transfer}} + \underbrace{\dot{F}_g \frac{dx_{H_2O(L)}}{dz} Cp_{H_2O(g)}(T_g - T_p)}_{\text{Energy variation of water vapor exchanged between the gas and the pellets}} + \underbrace{\dot{F}_g Cp_g \frac{dT_g}{dz}}_{\text{Gas: Heat flow in - heat flow out}} = \underbrace{0}_{\text{Heat accumulation}} \quad (11)$$

where h stands for the heat transfer coefficient, $\ddot{A}_p$ the heat exchange area per volume, T_g the gas temperature, T_p the pellet temperature, $\dot{F}_g$ the superficial gas flow, $\frac{dx_{H_2O(L)}}{dz}$ the pellet humidity variation inside the element dz, $Cp_{H_2O(g)}$ the specific heat capacity of water in gaseous state, and Cp_g the gas specific heat capacity. For the pellets, the energy balance for the same cell with a length dx is:

$$\underbrace{-\dot{F}_p(Cp_p + x_{H_2O(l)} Cp_{H_2O(L)})\frac{dT_p}{dx}}_{\text{Pellets: Heat flow in - heat flow out}} + \underbrace{\dot{F}_p \frac{dx_{H_2O(L)}}{dz}\Delta H_{H_2O}(T_p)}_{\text{Energy variation caused by the water evaporation or condensation}} + \underbrace{\sum \ddot{F}_i^{rx} \Delta H_i^{rx}(T_p)}_{\text{Energy variation caused by the chemical reactions}} \quad (12)$$

$$\underbrace{-h\ddot{A}_p(T_g - T_p)}_{\text{Convective heat transfer}} = \underbrace{0}_{\text{Heat accumulation}}$$

where $\dot{F}_p$ is the superficial pellet flow, Cp_p the specific heat capacity of the pellets, $x_{H_2O(L)}$ the water content of the pellets, $Cp_{H_2O(L)}$ the specific heat capacity of water in liquid state, $\Delta H_{H_2O}(T_p)$ the enthalpy variation for water evaporation at T_p, $\ddot{F}_i^{rx}$ the mass of the reactive specie i that reacts per unit of time and volume, and $\Delta H_i^{rx}(T_p)$ the enthalpy variation for the reactive specie i at T_b. Eqs. (11) and (12) are solved sequentially for each cell as shown in Fig. 3 where the superscript *i* represents the input and the superscript *o* the output.

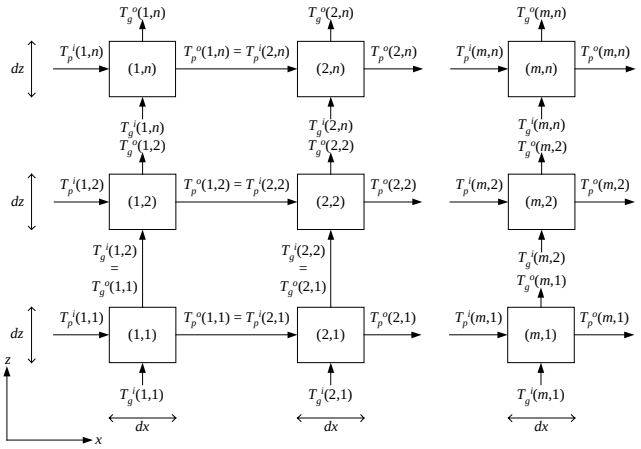

Figure 3: Moving cooling bed schematization.

The properties of the sintered product mainly depend on the temperature profile of the bed in the combustion zone. The pellet quality is simulated by an empirical model proposed by Batterham [11] which describes the development of strength Q in pellets submitted subject to a time-temperature profile $T(t)$ by:

$$\frac{dQ}{dt} = f(Q,T) = \kappa(Q_f - Q) \quad (13)$$

where κ is a temperature dependent rate parameter and Q_f is the final quality that would be obtained after a long period of sintering at temperature T. The rate term κ is temperature dependent through an Arrhenius type expression:

$$\kappa = \frac{A_0}{T}\exp\left(\frac{-E}{T}\right) \quad (14)$$

where A_0 is a constant for a given pellet composition. In order to define an appropriate form for Q_f, it is necessary to account for the rapid rise in quality that occurs once T exceeds a value T_L, which corresponds to the liquid phase apparition in fluxed pellets. It is also necessary to consider that the pellet quality decreases above a critical temperature (T_C), due to a vitrification phenomenon [12]. Fig. 4 shows the final quality model given by

$$Q_f = \nu + \frac{\beta}{1+\exp\left(\frac{-(T-T_L)}{\gamma}\right)} \quad T \le T_C$$
$$Q_f = \nu + \frac{\beta}{1+\exp\left(\frac{-(T-T_L)}{\gamma}\right)} - \frac{\delta}{1+\exp\left(\frac{-(T-T_c-\psi)}{\varphi}\right)} \quad T > T_C \qquad (15)$$

Therefore, the final equation has ten adjustable parameters: $A_0, E, \nu, \beta, \delta, \gamma, \varphi, \psi, T_L,$ and T_C. These parameters vary with the nature and amount of additives, the ore type, and the balling conditions. Once the ten parameters are determined, the state equation can be used to integrate along any time-temperature $T(t)$ profile by solving:

$$\int_{Q(t=0)}^{Q(t=t)} dQ = \int_{t=0}^{t=t} \frac{\kappa}{T} \exp\left(\frac{-E}{T}\right)(Q_f - Q)dt \,. \qquad (16)$$

The proposed model was calibrated on an empirical model gathering results of a data base obtained through extensive pilot pot-grate tests [7,12]. The compression strength (σ) is the pellet quality indicator chosen.

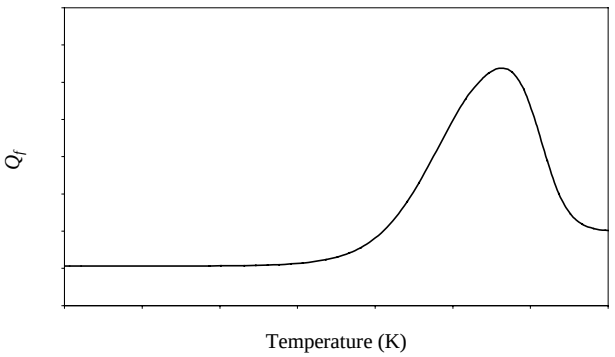

Figure 4: Final pellet quality.

B. Optimization problem

The operation point of the induration furnace is defined by the following ten independent variables which form the vector $\boldsymbol{U}$. The pressure variation at the fan boundaries (dP_{V1} to dP_{V5}) can be modified with the fan shutter openings. The quantity of fuel consumed by the burners can also be manipulated ($F_{m,PC}$, $F_{m,C1}$, and $F_{m,C2}$). Finally, the grate speed and the bed height can also be altered.

For the induration furnace, the purpose of the RTO algorithm is to reduce the fuel consumption by time unit, which is the most important production cost, at a given production level defined by two independent variables that are the moving grate speed (v) and the bed height (H). The optimization criterion is then:

$$\min_{\boldsymbol{U}} J = \min_{\boldsymbol{U}} \left[F_{m,PC} + F_{m,C1} + F_{m,C2}\right] \qquad (17)$$

Several constraints should be respected during the pellet production. The minimum pellet quality is one of the most important inequality constraints. As mentioned before, the clients require pellets of minimum compression strength. All cooked pellets do not exhibit the same compression strength since they have not been exposed to the same time-temperature profiles. As a consequence, their mechanical properties follow a probability distribution. Therefore, there are two inequality constraints on the product quality attributes (PQAs): the mean of the pellet compression strength ($\overline{\sigma}$) must be larger than 260 kg/pellet and less than 5% of the produced pellets should have compression strength smaller than 150 kg/pellet (σ_{min}):

$$\begin{aligned} &\overline{\sigma} \ge 260 \text{ kg/pellet} \\ &\sigma_{min} \ge 140 \text{ kg/pellet} \end{aligned} \qquad (18)$$

The other inequality constraints are security and operational constraints. Operational constraints are applied on the independent variables of the optimization problem. These inequality constraints are the actuator limits:

$$\begin{aligned} &4500 \le dP_{V1} \le 5500 \text{ (Pa)} \quad &&0 \le F_{m,PC} \le 0.053 \text{(kg/s)} \\ &3100 \le dP_{V2} \le 3900 \text{ (Pa)} \quad &&0.04 \le F_{m,C1} \le 0.11 \text{(kg/s)} \\ &4000 \le dP_{V3} \le 5000 \text{ (Pa)} \quad &&0.62 \le F_{m,C2} \le 0.8 \text{ (kg/s)} \\ &4700 \le dP_{V4} \le 5700 \text{ (Pa)} \quad &&2.6 \le v \le 3 \text{ (m/min)} \\ &1600 \le dP_{V5} \le 2000 \text{ (Pa)} \quad &&0.47 \le H \le 0.53 \text{ (m)} \end{aligned} \qquad (19)$$

Security constraints are applied to measured variables (with hard or soft sensors):

$$\begin{aligned} &P_1 \le -100 \text{ Pa} \quad &&T_1 \le 300 \text{ °C} \\ &P_2 \le -100 \text{ Pa} \quad &&T_{11} \le 300 \text{ °C} \\ &P_4 \le 2000 \text{ Pa} \quad &&T_p^o \le 100 \text{ °C} \\ &P_6 \le 2000 \text{ Pa} \end{aligned} \qquad (20)$$

where T_p^o is the average pellet temperature at the end of the second cooling zone.

C. Reduced models

The optimization problem of the induration furnace is only characterized by inequality constraints on $\boldsymbol{X}$ (Eqs. (18) and (20)). There is no equality constraint $\boldsymbol{R}_{SP}$. Furthermore, the criterion J is an explicit linear function of $\boldsymbol{U}$, then only the operators $\boldsymbol{P}$ and $\boldsymbol{P}_M$ are required in the IMC-optimization scheme (Figure 5). The operator $\boldsymbol{P}$ is the induration furnace simulator itself.

The reduced models were calibrated on data recorded from running the induration furnace simulator at various operating points and normalized according to Eq. (6). A

central composite design was done to select the operating points for the identification process. Central composite designs are response surface designs that can fit a full quadratic model. Usually, the optimum on an optimization problem is constrained. Thus, limit values are important when designing the process model. A faced design was chosen since it has three levels per factor and has points on the faces of the cube.

The operator $\boldsymbol{P}_M$ used to predict the constrained normalized dependent variables (Eq. 20) and PQAs (Eq. 18) is as followed

$$\boldsymbol{X}_M^n = \sum_{i=1}^{10} b_{x_M^n,i} u_i^n + \sum_{i=1}^{10}\sum_{j\geq i}^{10} b_{x_M^n,ij} u_i^n u_j^n \qquad (21)$$

where $\boldsymbol{X}_M^n$ are the normalized $\boldsymbol{X}_M$ variables and u^n the normalized independent variables $\boldsymbol{U}$. Only the parameters b that are significantly different from zero are kept.

To model adequately the PQAs as a function of the independent variables $\boldsymbol{U}$, two different linear models have to be used since the final quality of the pellets (Q_f) increases with the temperature until a critical temperature (T_C) is reached. For temperatures higher than T_C, Q_f decreases with a temperature increase. The gas temperature T_1, which is a dependent variable, is used as an indicator of the pellet temperature. When the estimated T_1 is smaller than 345°C, the first model is used. The second model is otherwise preferred.

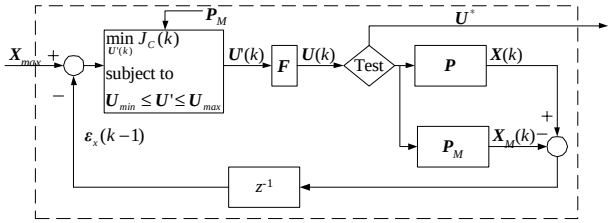

Figure 5: IMC-Optimization structure for the induration furnace.

IV. Results

All optimizations are performed with the Matlab function *fmincon*. The termination tolerance on $\boldsymbol{U}$ is set to 10^{-2}. The parameter η in the IMC-Optimization scheme is also set to the same value. The parameter ρ of the low-pass filter is set to 0.5. A larger value of ρ increases the robustness to model mismatch between $\boldsymbol{P}$ and $\boldsymbol{P}_M$ but slows down the convergence. The desired production rate is set to 5.41 m^3/min.

The IMC-Optimization (IMCop) presented in Section 2 will be compared to a direct optimization of criterion (1) subject to constraints defined by Eq. (2). The initial guess for the IMCop is zero for all normalized variables. The direct optimization procedure is run with two different initial guesses. The first direct optimization (Nlop1) use the same initial guess as the IMCop. The second direct optimization (Nlop2) uses as initial guess the result of the optimization of Eq. (3) with respect to Eq. (4) using $\boldsymbol{X}_{max-C} = \boldsymbol{X}_{max}$. This initial guess corresponds to the optimization based on $\boldsymbol{P}_M$, which is in fact the result of the first iteration of the IMC-Optimization. Table 1 compares the results of the three optimization procedures. The IMCop method needs to run the first principles simulator only 7 times while it was respectively run 150 times and 68 times for NLop1 and NLop2 respectively.

Table 1: Induration furnace optimization.

Parameter	NLop1	NLop2	IMCop
Fuel consumption (kg/s)	0.75	0.67	0.69
Production level (m^3/min)	2.41	2.41	2.41
Number of runs of the nonlinear model	150	68	7
Time required (s)	4.56E+4	2.10E+4	2.87E+3
dP_{V1} (Pa)	5440	4500	4860
dP_{V2} (Pa)	3900	3900	3900
dP_{V3} (Pa)	5000	4960	5000
dP_{V4} (Pa)	5700	5700	4700
dP_{V5} (Pa)	1600	2000	1600
$F_{m,PC}$ (kg/s)	0	0	0
$F_{m,C1}$ (kg/s)	0.04	0.04	0.04
$F_{m,C2}$ (kg/s)	0.71	0.63	0.65
H (m)	0.52	0.52	0.50
v (m/min)	2.62	2.6	2.69
$\overline{\sigma}$ (kg/pellets)	260	270	270
$\overline{\sigma}_{min}$ (kg/pellets)	160	140	140
Constraints hit	dP_{V2}, dP_{V3}, dP_{V4}, dP_{V5}, $F_{m,PC}$, $F_{m,C1}$, $\overline{\sigma}$	dP_{V1}, dP_{V2}, dP_{V4}, dP_{V5}, $F_{m,PC}$, $F_{m,C1}$, v, $\overline{\sigma}_{min}$	dP_{V2}, dP_{V3}, dP_{V4}, dP_{V5}, $F_{m,PC}$, $F_{m,C1}$, $\overline{\sigma}_{min}$

The response surface of the optimization problem exhibits local minima, which leads to various solutions depending on the starting point and the optimization algorithm. The local minima of both algorithms are not necessarily located at the same operating points. The true minimum cost function value is obtained with NLop2. However, for the

same starting point, the optimum obtained with the IMCop is smaller than the one obtained with NLop1. Finally, the difference between the NLop2 and IMCop optima is small comparatively to the model errors. The actual goal being the optimization of the real process and not its model, the IMC optimization algorithm is interesting for real-time optimization applications due to its small computational costs despite the algorithm may converge to a slightly biased solution.

For the same production level and pellet quality, the energy consumption is reduced if the moving grate speed is low and the bed height is high. In fact, the lowest energy consumption is obtained when the bed speed hits its minimum constraint. Moreover, the results show, from an economic point of view, that it is better to reduce the fuel consumption in the pre-cooking and first cooking zones. Therefore, the pellet sintering occurs mainly in the second cooking zone.

The coke combustion is the most important energy source. A low moving grate speed allows more time for the coke combustion, thus giving more energy to sinter the pellets in the bottom layers of the bed. The energy released by the coke combustion gives enough energy to sinter the pellets and is recovered by the gas flow and therefore it is unnecessary to heat the pellets in the pre-cooking and cooking zones because of the adequate coke combustion. The fuel injected in the burners in the second cooking zone is only used to start the coke combustion.

V. Conclusion

Induration furnaces are complex and interactive processes that are expensive to run due to their high-energy consumption. Despite optimization is essential in the actual economic context, it is difficult to determine intuitively the best operating point. A reliable process model is necessary for process optimization. However, the required parameter-distributed models are too computationally expensive for a real-time optimization application. Therefore, the IMC-optimization algorithm is an interesting alternative for this type of process. The IMC-optimization algorithm allows the user to use a simple optimization algorithm, is easy to implement and tune, and exhibits fast convergence. For the induration furnace, the performance obtained is as good as the one obtained with the nonlinear optimization algorithm, but the most important point is that the implementation in the real plant is now possible. Finally, the IMC-optimization algorithm can be used for other computationally expensive data analysis such as model updating and nonlinear model-based predictive control.

The optimization results give guidelines for the induration furnace operation. From an economic point of view, it is better to reduce the fuel consumption in the pre-cooking and first cooking zones. Also, for the same production level and pellet quality, the energy consumption is reduced if the moving grate speed is low and the bed height is high.

VI. Acknowledgements

The authors are grateful to QCM (Quebec-Cartier Mining), NSERC (Natural Science and Engineering Research Council of Canada), and FQRNT (Fonds québécois de la recherche sur la nature et les technologies) for their financial support and authorization to publish.

VII. References

[1] Desbiens, A. and Shook, A.A., IMC-Optimization of a Direct Reduced Iron Phenomenological Simulator, *4th ICCA'03*, Montreal, Canada, 2003, accepted.

[2] Chen, C.Y. and Joseph, B., On-Line Optimization Using a Two-Phase Approach: An Application Study, Ind. Eng. Chem. Res., **26**, 1987, pp.1924-1930.

[3] Nocedal, J. and Wright, S.J., Numerical optimization, Springer, New York, 1999.

[4] Garcia, C.E. and Morari, M., Internal Model Control. 1. A Unifying Review and Some New Results, *Ind. Eng. Chem. Process. Des. Dev.*, **21**, 1982, pp. 308-323.

[5] Bernier, H. and Lebel, D., Pellet Quality Improvements at Wabush Mines, *Proc. ICSTI / Iron Making Conf.*, Toronto, 1998, pp.987-992.

[6] Wynnyckyj, J.R. and Batterham, R.J., Iron Ore Sintering and Pellet Induration Processes, *4th Int. Symposium on Agglomeration*, Toronto, 1985, pp.957-994.

[7] Kuçukada, K., Thibault, J., Hodouin, D., Paquet G. and Caron, S., Modelling of a Pilot Scale Iron Ore Pellet Induration Furnace, *Can. Metallurgical Quarterly*, **33**, 1994, pp.1-12.

[8] Bébé Ekongolo, S., Makni, S. and Hodouin, D., Global Flow Distribution Simulation for Iron Ore Pellets Induration, *38th Conf. of Metallurgists*, CIM, Quebec, 1999, pp.239-253.

[9] Osborne, W.C., Fans, 2nd Edition, Pergamon Press Ltd, Oxford, 1977.

[10] Afzal, M. and Cross, M., Mathematical Modelling of the Gas Flow Distribution in Iron Ore Pellet Induration System, *10th PTD Conf.*, 1992, pp.367-374.

[11] Batterham, R.J., Modeling the Development of Strength in Pellets, *Metallurgical Trans. B*, 17B, 1986, pp.479-485.

[12] Research team, Modèles des propriétés physiques et métallurgiques – SIMBOUL intégré V3.0, COREM, Quebec City, October 1998.